Edelweiss Applied Science and Technology
ISSN: 2576-8484
Vol. 9, No. 5, 2656-2669
2025
Publisher: Learning Gate
DOI: 10.55214/25768484.v9i5.7581

Investigation of solar air heater optimization with spherical Rib

Abduljabbar Muttair Ahmed[1*]
[1]Electromechanical Engineering Department, University of Technology- Iraq, Baghdad, 10068, Iraq;
abduljabbar.m.ahmed@uotechnology.edu.iq (A.M.A.).

Abstract: One clean and environmentally beneficial energy source is solar power. Transparent collector solar air heaters (SAH) are a prime example of the technology currently being researched for use in warming homes and offices. Spherical ribs with three groups of diameters (2, 2.5, and 3 mm) and a relative pitch P/e = 12 for each one. Heat flux from solar energy is 1000 W/m2 for both shapes if a smooth absorbent plate and roughened rib are used. The flow rate at the inlet is determined from the range of values for the Reynolds number (5000 – 15000). A k-ε turbulence model and ANSYS Fluent have been used for the numerical simulation. The Nusselt number, friction factor, and heat transfer coefficient values have all been determined. The velocity vector and temperature contour give the flow behavior inside the collector. For the Reynolds number range of 5000–15000, the thermohydraulic factor performance (THPF) can be enhanced up to 2.3. Including spherical ribs across the absorber plate improves the SAH's thermal performance. The suggested artificially roughened surface is advantageous for low domain Reynolds numbers because the maximum enhancement of the THPF value has been found in a region of low Reynolds numbers.

Keywords: *Nusselt number, Solar air heater SAH, Spherical rib, Thermo-hydraulic factor.*

1. Introduction

The benefit of studying solar air heater (SAH) is of high importance because it is used in many applications like agriculture and heating homes in winter, leading to a reduction in the consumption of electric power. Researchers have done many numerical simulations and experimental investigations for roughened ribs. Tow configuration, the first one with the constant value of pitch (p) and different value of sphere diameter. A second one with a constant diameter and different types of pitch (p). The influence of relative roughness on performance has been numerically studied Manjunath, et al. [1]. Solar air heater with a different of tiny dimples studded to simulate a dimple using ANSYS. Using V-miniature dimples demonstrated the best thermohydraulic performance at Re above 8750 at a 45° angle, while a 90° transverse broken-miniature with dimple demonstrated the best thermohydraulic performance at Renolds number (Re) below 10,000. This has been done by Arya, et al. [2]. Al Ghuol, et al. [3] have investigated solar air collectors conducted with a spherical shape phase change material unit to enhance the performance of thermal storage efficiency and minimize time charge. Prakash and Saini [4] carried out experimental work for an incline rib with a spherical dimple to investigate the flow of air and heat characteristics. The enhancement of Nusselt number led to increases in the fiction factor by using roughened rib. Perwez and Kumar [5] experimentally investigated when the absorber plate collector has a similar diameter to the spherical dimple. The instantaneous efficiency of the solar air heater increases from 23.45 % to 35.5 %. To explore the impact of artificially roughened surfaces on heat transmission and friction factor in solar air heaters, angular dimples produced on absorption plates have been carried out by Sethi and Thakur [6]. The roughened duct containing spherical balls in an inclined line conducted as an experimental rig to drive the governing equations depending on the result

History: Received: 10 March 2025; Revised: 23 April 2025; Accepted: 28 April 2025; Published: 27 May 2025
* Correspondence: abduljabbar.m.ahmed@uotechnology.edu.iq

generated from outdoor conditions has been investigated by Murmu, et al. [7]. The obstacles may be used as a spherical shape on a heated wall for different Reynolds number ranges to examine thermal characteristics and select the optimization value for this configuration have been done by Bhardwaj, et al. [8]. The thermohydraulic performance of solar collectors with perforated baffles attached to one wall in a rectangular duct has been experimentally investigated. The improvement in the presence of perforated baffles is significant in factor friction and Nusselt number with the smooth duct [9]. A CFD simulation of SAH attached with an absorber plate and circular ribs is analyzed. A linear stepwise regression approach is used to reduce the obtained data into correlations. All statistics for friction factor and Nusselt number are predicted within 5% relative absolute deviation using the developed formulae for intentionally roughened solar air heaters [10]. As mentioned earlier, simple SAH is less efficient than many thermal systems. In this regard, some studies on improving heat transfer and building efficient SAH are in progress, including but not limited to, connecting different types of rib. The current work aims at numerical simulation using computational fluid dynamics (CFD) for a new artificial roughened surface to improve the SAH's thermohydraulic efficiency. In this study, three configurations of solar air heaters with different diameters and pitches for spherical ribs on the solar absorber have been investigated to improve the solar collector. Numerical analyses using computational fluid dynamics to test the effect of different types of spherical arrangement on heat transfer inside the air cavity with comparison by smooth solar air heater. The research covers the effect of diverse Reynolds numbers on the three configurations of the proposed SAH.

2. Mathematical Formulation

The three-dimensional airflow characteristics in the SAH are governed by firstly continuity, secondly momentum, and thirdly energy equations [11].

Continuity Equation

$$\nabla \cdot (\vec{u}) = S_m \tag{1}$$

Momentum Equation

The momentum equation in an inertial reference frame is expressed by.

$$\nabla \times (\rho \vec{u} \vec{u}) = -\nabla p + \nabla \cdot \bar{\bar{\tau}} + \rho \vec{g} + \vec{F} \tag{2}$$

Energy Equation

Turbulent heat transport is modeled using the concept of Reynolds' analogy to turbulent momentum transfer. The modeled energy equation is thus given by the following.

$$\frac{\partial}{\partial x_j}\left[u_i(\rho E + p)\right] = \frac{\partial}{\partial x_j}\left(k_{eff}\frac{\partial T}{\partial x_j} + u_i(\tau_{ij})_{eff}\right) + S_h \tag{3}$$

Where

$$(\tau) = \mu\left(\frac{\partial u}{\partial x} + \frac{\partial u}{\partial x}\right) - \frac{2}{3}\mu\frac{\partial u}{\partial x}\delta \tag{4}$$

Consequently, the significant target of this numerical simulation is to explore and examine the spherical rib that covers the full absorber plate in three groups of diameter from spherical ribs in the solar.

The factor of the performance of Thermohydraulic can be calculated by using the formula [12].

$$THPF = \frac{Nu_r/Nu_o}{(fr/f_o)^{1/3}} \tag{5}$$

3. Numerical Simulation and CFD Modeling

Investigating the solar air collector's roughened rib was done using a CFD. Depending on the existence of ribs, two designs for the solar air collector with a rectangular form and dimensions of 1.2 m by 0.03 m by 0.8 m have been evaluated. The smooth surface of the absorbent plate from copper in

Edelweiss Applied Science and Technology
ISSN: 2576-8484
Vol. 9, No. 5: 2656-2669, 2025
DOI: 10.55214/25768484.v9i5.7581

the first geometry with two walls of aluminum material, a glass for the roof surface, has been performed in a model as shown in Figure 1.

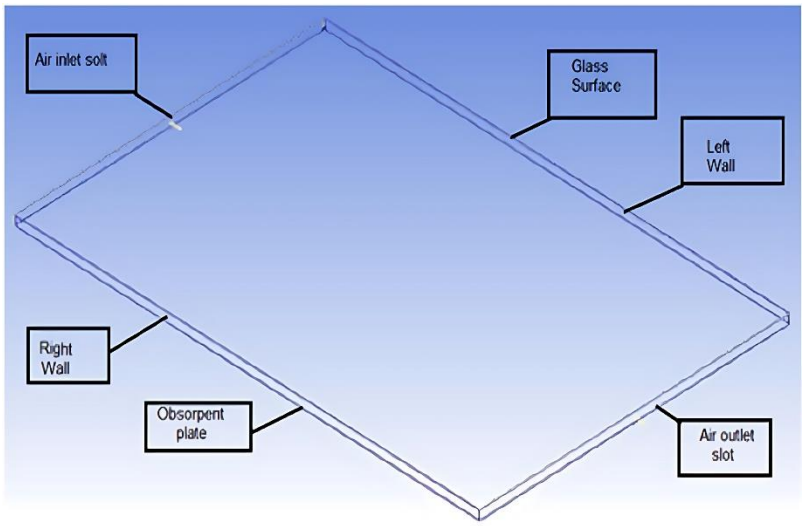

Figure 1.
Schematic diagram of the smooth surface of the collector.

In the second geometry, a spherical rib with three diameters (2, 2.5, and 3 mm) and relative pitch P/e = 12 for each one. Spherical ribs of copper material are present on an absorbent plate to increase the rate of absorption of sunlight compared to the smooth heater as shown in Figure 2.

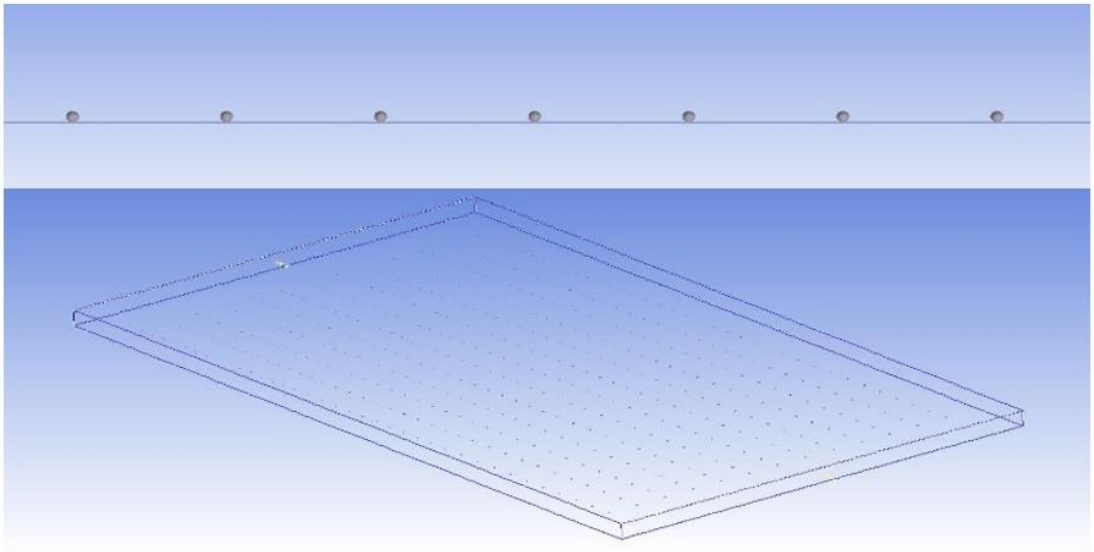

Figure 2.
Schematic diagram of the spherical rib of the collector.

Heat flux from solar energy is 1000 W/m^2 for both geometries. Airflow rates at the inlet of the solar air heater based upon Reynold's number were in the range of (5000 – 15000). The solving of continuity, energy, and momentum equations is done. The realizable k- ε (RKE) version of the

Edelweiss Applied Science and Technology
ISSN: 2576-8484
Vol. 9, No. 5: 2656-2669, 2025
DOI: 10.55214/25768484.v9i5.7581

turbulence model has been used to solve the governing equations. The simplest algorithmic type is used in the connection of pressure and velocity. The numerical solution was done by applying ANSYS fluent for the condition of steady state. Geometry preparation, node generation, and mesh generation are all included in the preparation. The type of mesh applied in the numerical procedure for a smooth surface without ribs has numerical (228000) elements and (252420) numerical nodes as is shown in Figure 3 whereas the computational grid employed for the numerical solution for spherical rib surface has numerical (3193889) elements and (3343246) numerical nodes as shown in Figure 4.

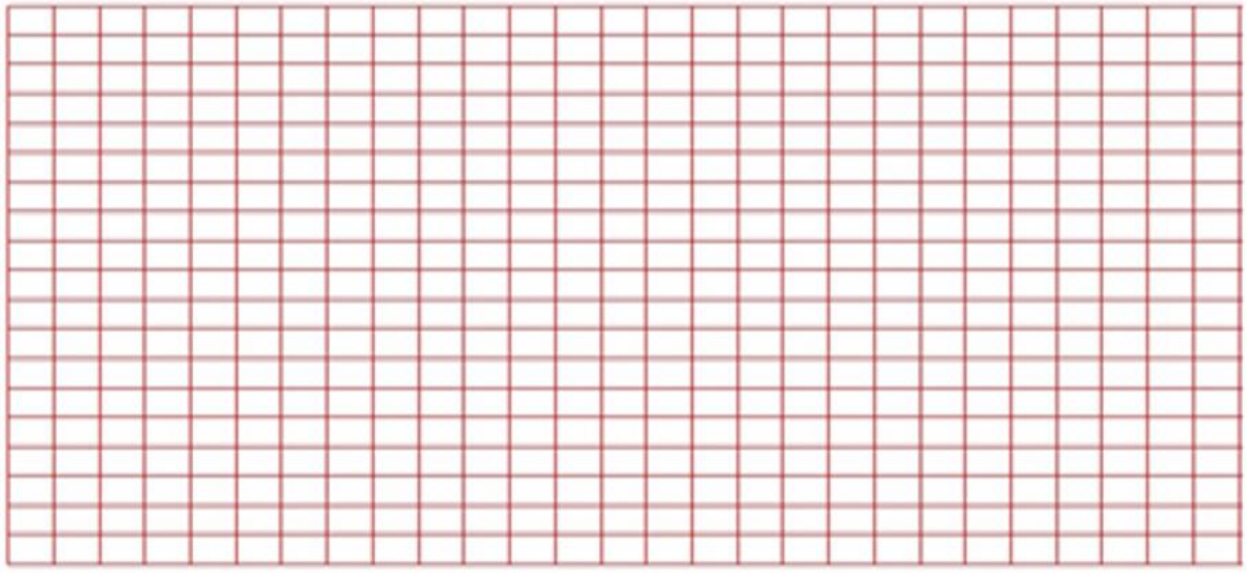

Figure 3.
Sample of mesh applied for the numerical procedure for a smooth surface.

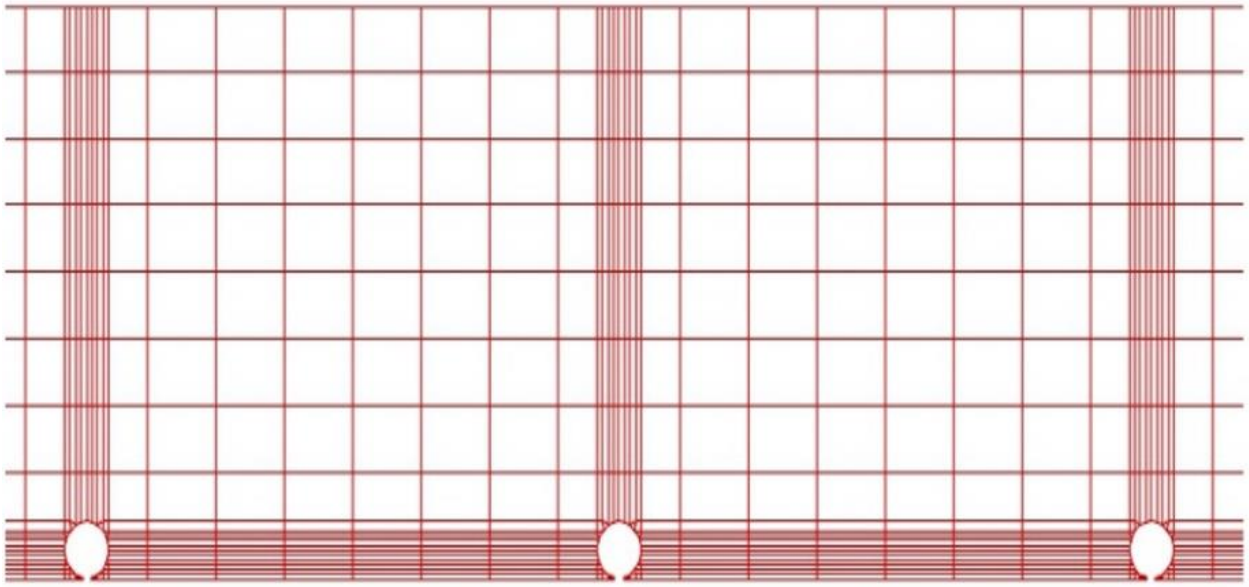

Figure 4.
Sample of mesh that was applied for the numerical procedure with a spherical rib.

Edelweiss Applied Science and Technology
ISSN: 2576-8484
Vol. 9, No. 5: 2656-2669, 2025
DOI: 10.55214/25768484.v9i5.7581

The finite volume approach is used to discretize the transport equations. The pressure-velocity coupling approach uses the SIMPLE algorithm. There are several options for presenting the findings of post-processing analysis, including contours, X-Y charts, and velocity vectors. Numerous factors, including velocity, temperature, and many more, may be analyzed using the options given.

4. Results and Discussion

4.1. Effect of changing Reynold's number on Nusselt number

Figure 5 depicts a typical average of variation for the Nusselt number as a function of the Reynolds number for both a spherical solar air heater (SSAH) and a smooth collector at (1000 W/m^2) solar intensity flux). The average Reynolds number has increased, which has increased the average Nusselt number owing to an increase in the kinetic energy of turbulent flow caused by an increase in the rate of dissipation, which results in greater turbulence intensity. Figure 5 also compares SSAH with a roughened surface to SAH with a flat surface. At all Reynolds numbers, the average Nusselt number of an SSAH with a roughened surface is greater than that of a solar air heater with a smooth surface. The Nusselt number is around (14) higher than that of the solar air collector with a flat surface.

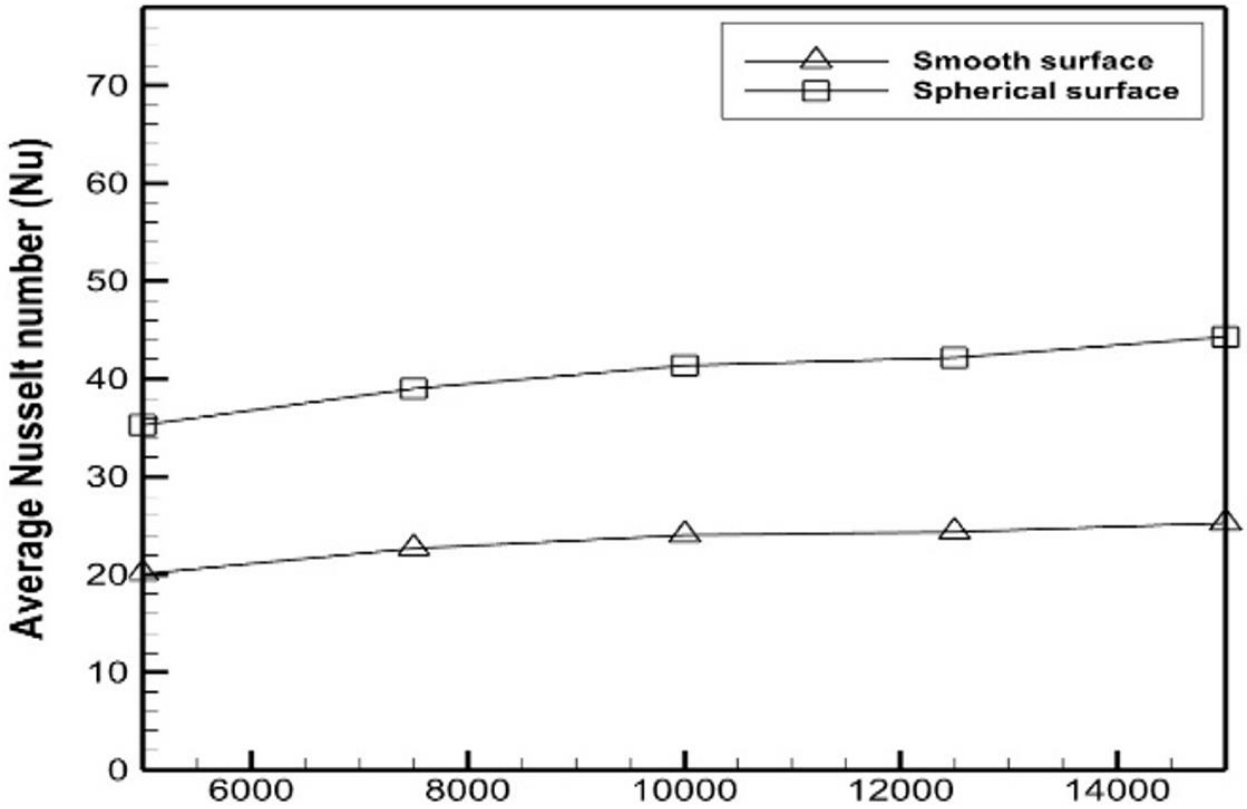

Figure 5.
The relationship between the average Nusselt number and the average Reynolds number.

4.2. Effect of Changing a Parameter on Friction Factor

The average factor of friction in a spherical solar air heater SSAH for roughened and smooth collectors can provide important information. Figure 6 depicts the influence of the Reynolds number on the friction factor for SAH for smooth and spherical surfaces. The graphic shows that the friction factor increases as the Reynolds number increases in both circumstances. The increase in friction factor is attributable to a decrease in the air boundary layer with a rising Reynolds number, resulting in a high

Edelweiss Applied Science and Technology
ISSN: 2576-8484
Vol. 9, No. 5: 2656-2669, 2025
DOI: 10.55214/25768484.v9i5.7581

number of ribs emerging into the main airflow. As a result, as the Reynolds number grows, so do the frictional losses. Furthermore, the figure shows that the least average friction factor value is (0.0015) for a smooth surface at Reynold number 5000 and the maximum value is (0.013) for a roughened surface at Reynold number 15000. This pattern of operation is predicted since the friction factor is less dependent on physical variables such as air density.

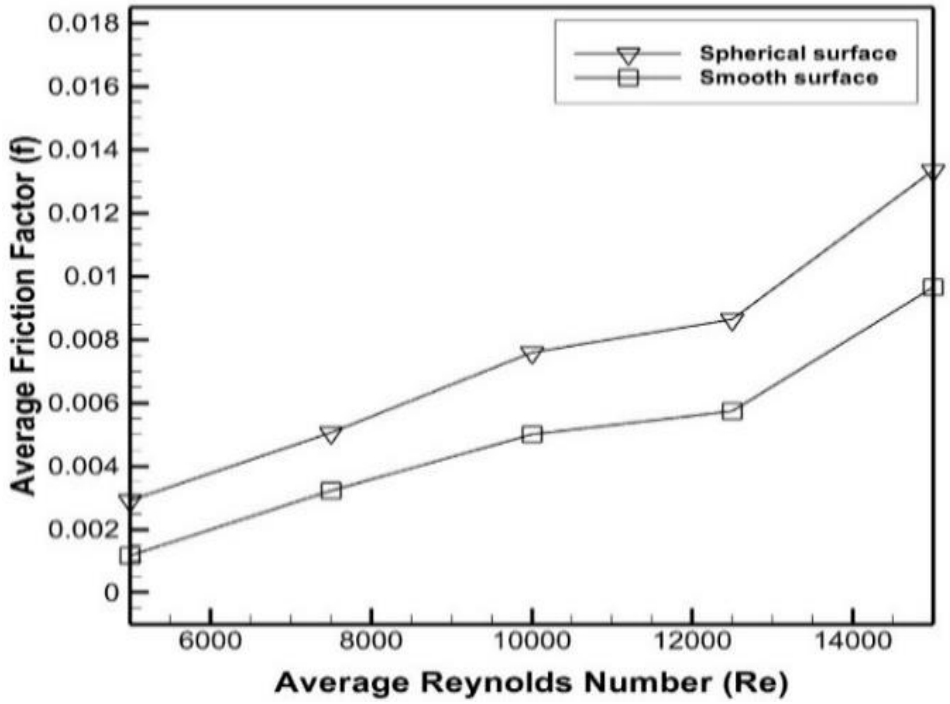

Figure 6.
The average friction factor varies with the average Reynolds number.

A minor surface alteration, specifically a spherical surface, can improve convective heat transmission. As seen in Figure 7. When SSAH with a spherical rib surface is compared to a smooth surface, the heat transfer coefficient increases with increasing Reynolds number. Furthermore, for a low Reynold number, the rising value for the coefficient of heat. Transmission is roughly 1.1 between smooth and roughened surfaces. As a result, as the sun intensity flux increases, so does the heat transfer coefficient

Edelweiss Applied Science and Technology
ISSN: 2576-8484
Vol. 9, No. 5: 2656-2669, 2025
DOI: 10.55214/25768484.v9i5.7581

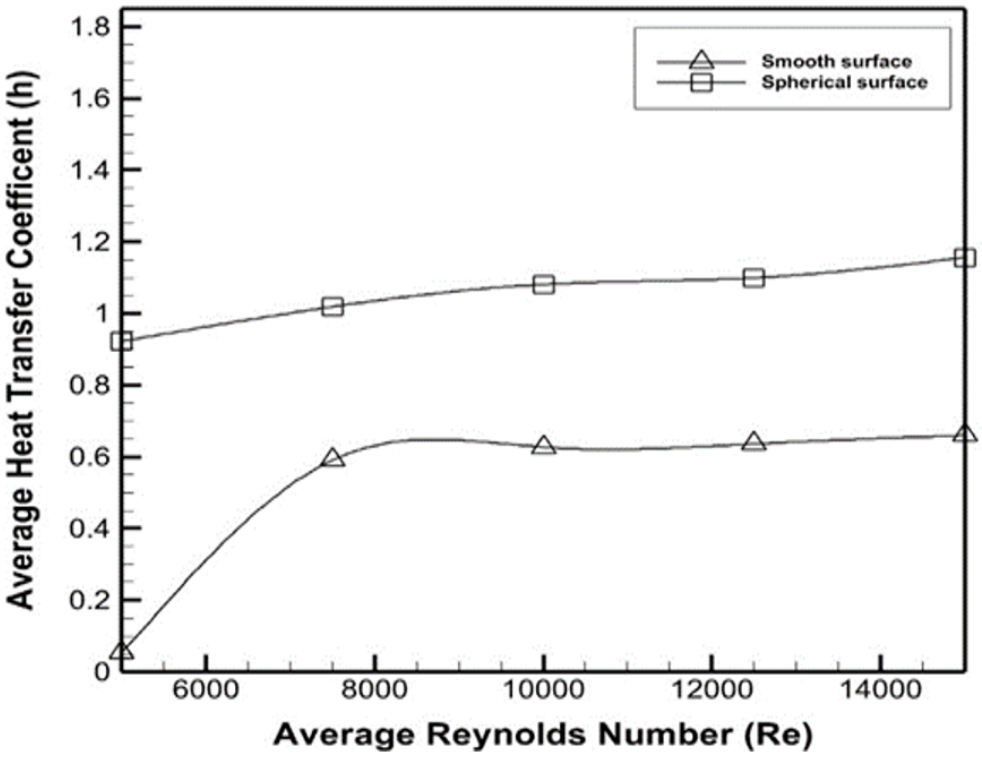

Figure 7.
The average heat transfer coefficient varies with the average Reynolds number.

4.3. Effect of Changing Reynolds Number on Temperature Distribution

For SAH with a smooth surface, the flow pattern is displayed as the velocity vector is measured at z plane = 0.4 m. Figure 8 depicts the velocity vector for Reynold numbers (5000 and 15000) and it is obvious that the intensity of the velocity vector when Reynold number 5000 is smaller than the intensity of the velocity vector when Reynold number 15000.

Edelweiss Applied Science and Technology
ISSN: 2576-8484
Vol. 9, No. 5: 2656-2669, 2025
DOI: 10.55214/25768484.v9i5.7581

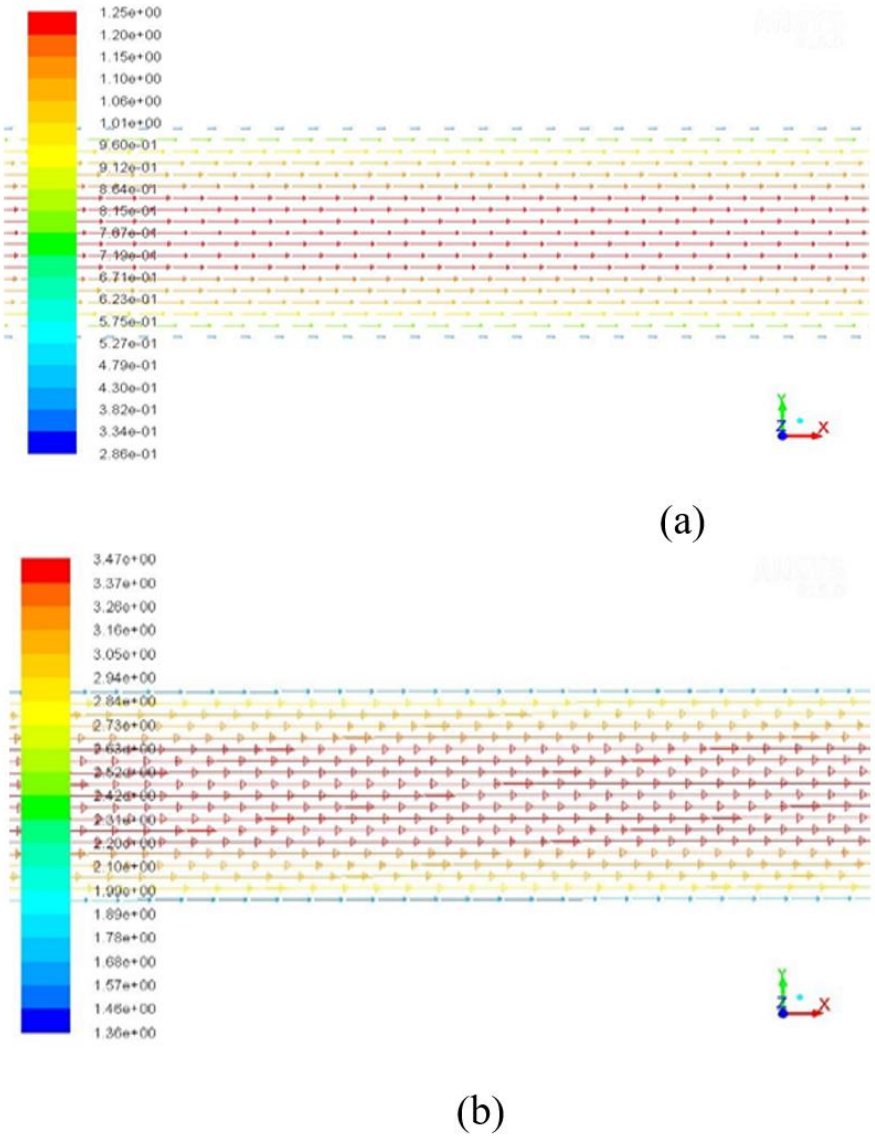

Figure 8.
Velocity vector for the smooth solar heater at midplane z=0.4 m (a) Re=5000 (b) Re= 15000.

Figure 9 illustrates the temperature contour at plane Y = 0.15 m on a flat surface with Reynold numbers of 5000 and 15000, demonstrating that the temperature is greater when the Reynolds number is 5000 than when the Reynolds number is 15000. This is because when the Reynolds number is low, the impact of mixing cold and hot air is reduced. As a result, if the Reynolds number is low, the rise in the average Nusselt number is reduced.

Edelweiss Applied Science and Technology
ISSN: 2576-8484
Vol. 9, No. 5: 2656-2669, 2025
DOI: 10.55214/25768484.v9i5.7581

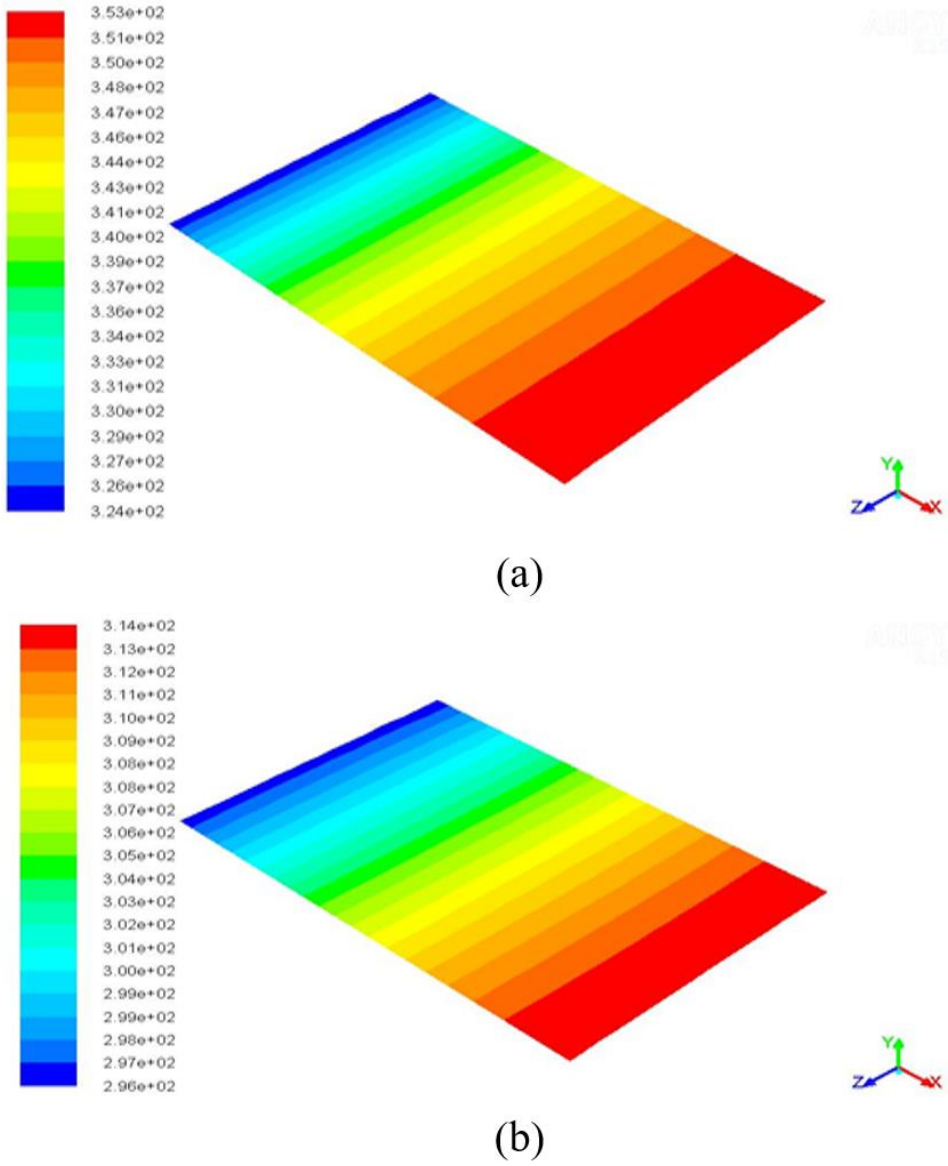

Figure 9.
Temperature contour for smooth solar air heater at midplane Y=0.15 m (a) Re=5000 (b) Re= 15000

Figure 10 shows the velocity vector for SSAH with roughened rib surface at z plane = 0.4 with Reynold number (5000 and 15000).

Obstructions generated below the ribs by Reynold number 5000 are weaker than obstructions generated by Reynold number 15000. The height and breadth of the ribs are crucial and have an effect on the outer flow of air; they also play a key role in determining the demand for design capacity in such a kind of energy system.

Edelweiss Applied Science and Technology
ISSN: 2576-8484
Vol. 9, No. 5: 2656-2669, 2025
DOI: 10.55214/25768484.v9i5.7581

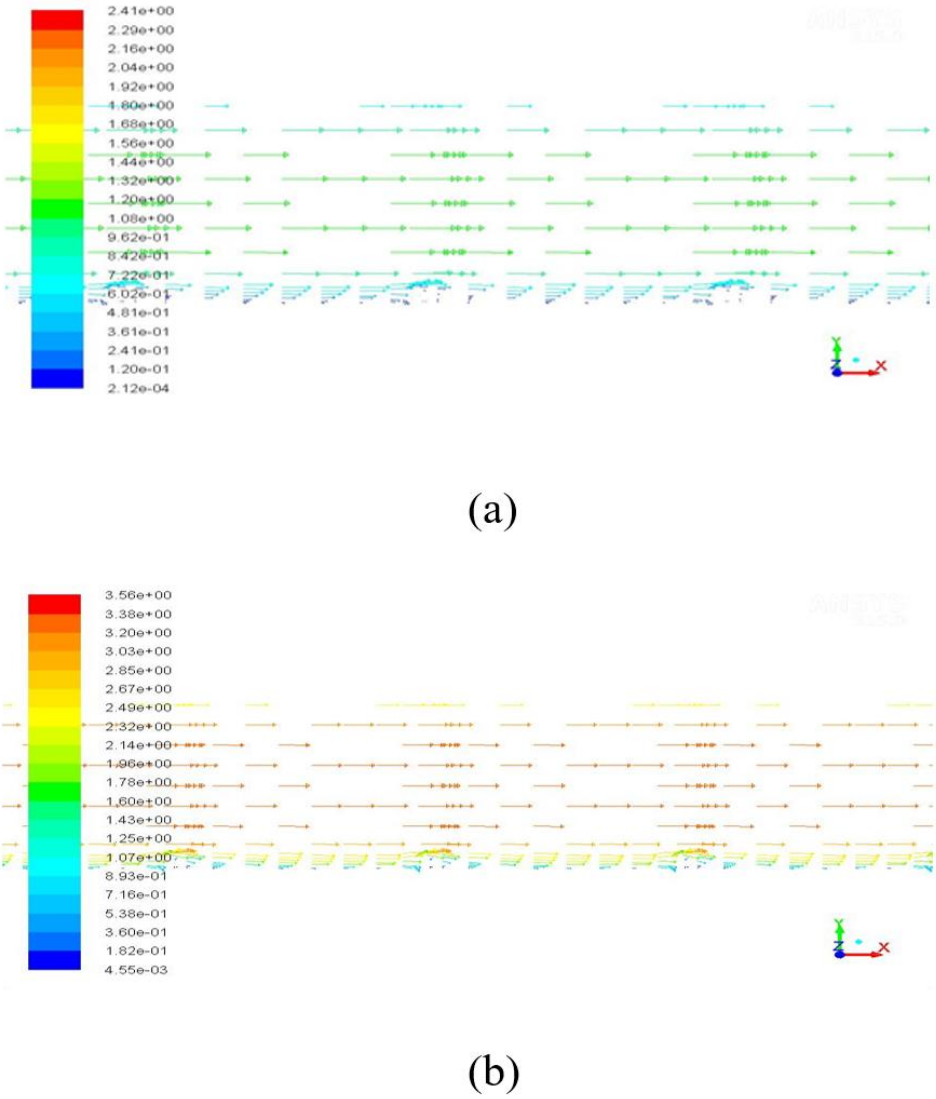

Figure 10.
Velocity vector for a solar heater with spherical rib at midplane z=0.4 m (a) Re=5000 (b) Re= 15000

The temperature contour depicts the temperature distribution when Reynold number 15000 is smaller than Reynold number 5000 as a result of the strong blockage formed behind the ribs, as seen in Figure 11.

Edelweiss Applied Science and Technology
ISSN: 2576-8484
Vol. 9, No. 5: 2656-2669, 2025
DOI: 10.55214/25768484.v9i5.7581

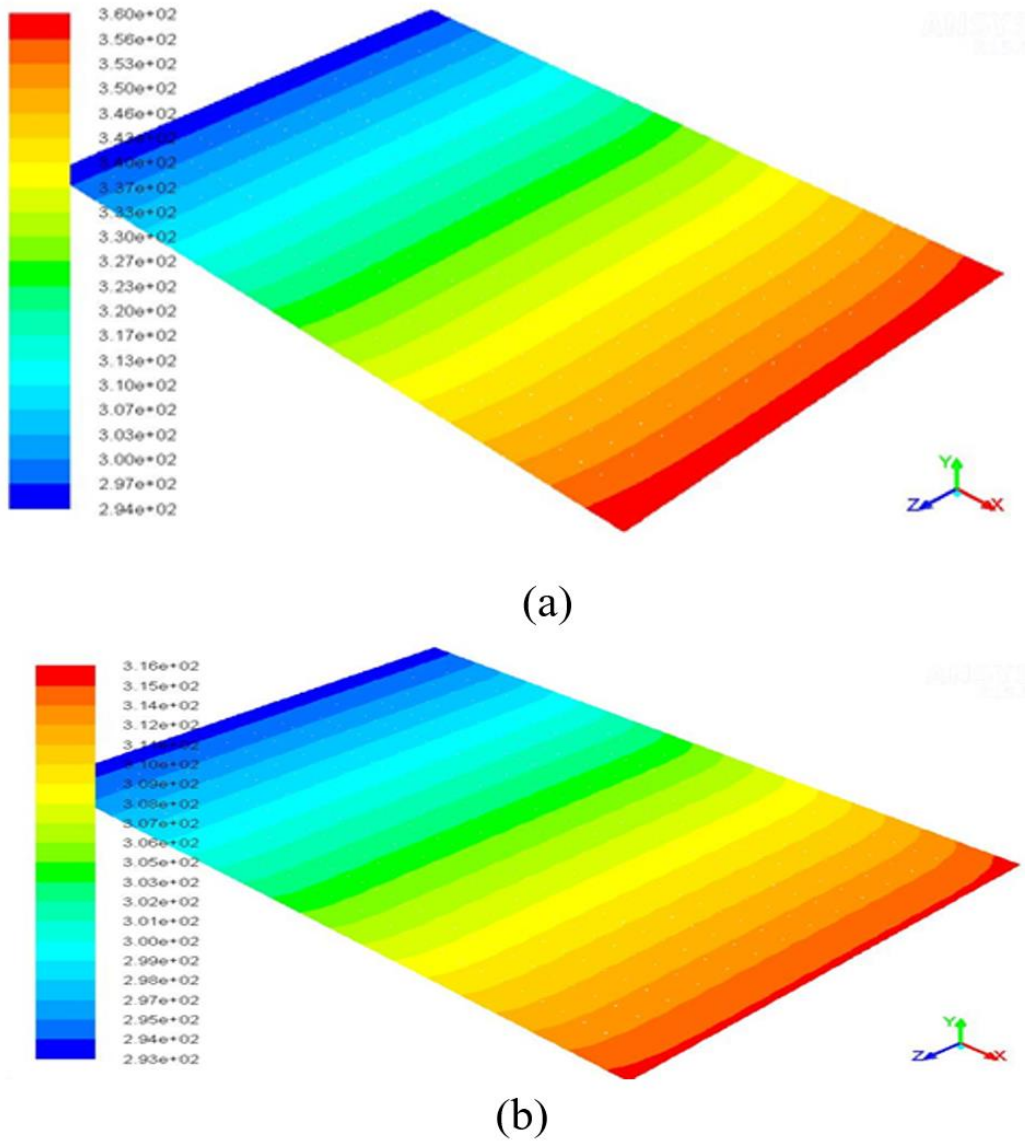

Figure 11.
Temperature contour for spherical rib solar air heater at midplane Y=0.01m (a) Re=5000 (b) Re= 15000.

4.4. Effect of Changing Reynold's Number on THPF

The placement of a spherical rib on the SSAH surface causes the laminar sublayer to disintegrate while also operating the surface flow layer. Additionally, the ribs induce turbulent flow, which increases heat transfer between the surface and the air moving over it. The height and breadth of the ribs are crucial and have an effect on the outer flow of air; they also play a key role in determining the demand for design capacity in such a kind of energy system. The space between the ribs is also significant and has an impact on the recirculation flow and eddies that occur behind the ribs. The use of a relatively high artificial rib increases the pressure drop and hence the coefficient of friction.

As a result, the artificial rib should be chosen in such a way that it generates turbulent flow near the surface, i.e. in the sublayer area. The selection of a relatively broad-width artificial rib with a relatively big space between ribs is related to a greater rate of heat transfer than the rise in the quantity of friction losses component in the current case study. It is critical to analyze the enhanced performance as a whole

Edelweiss Applied Science and Technology
ISSN: 2576-8484
Vol. 9, No. 5: 2656-2669, 2025
DOI: 10.55214/25768484.v9i5.7581

to determine the greatest performance of a current roughened solar air collector and compare it to the cases under the pupil. Some researchers were given a coefficient known as the Thermohydraulic performance factor (THPF) to quantify the performance of the artificial rib above the surface of the solar air collector. The THPP factor reaches its maximum value of 2.3 when the solar intensity flux is 1000 and the Reynolds number is about 5000. As a result, it is plausible to assert that the proportions and arrangement of an artificial rib as it currently exists have some profit potential. To provide a comprehensive overview of how the suggested artificial rib's use will impact the thermohydraulic factor THPF, all operational parameters are shown in Figure 12.

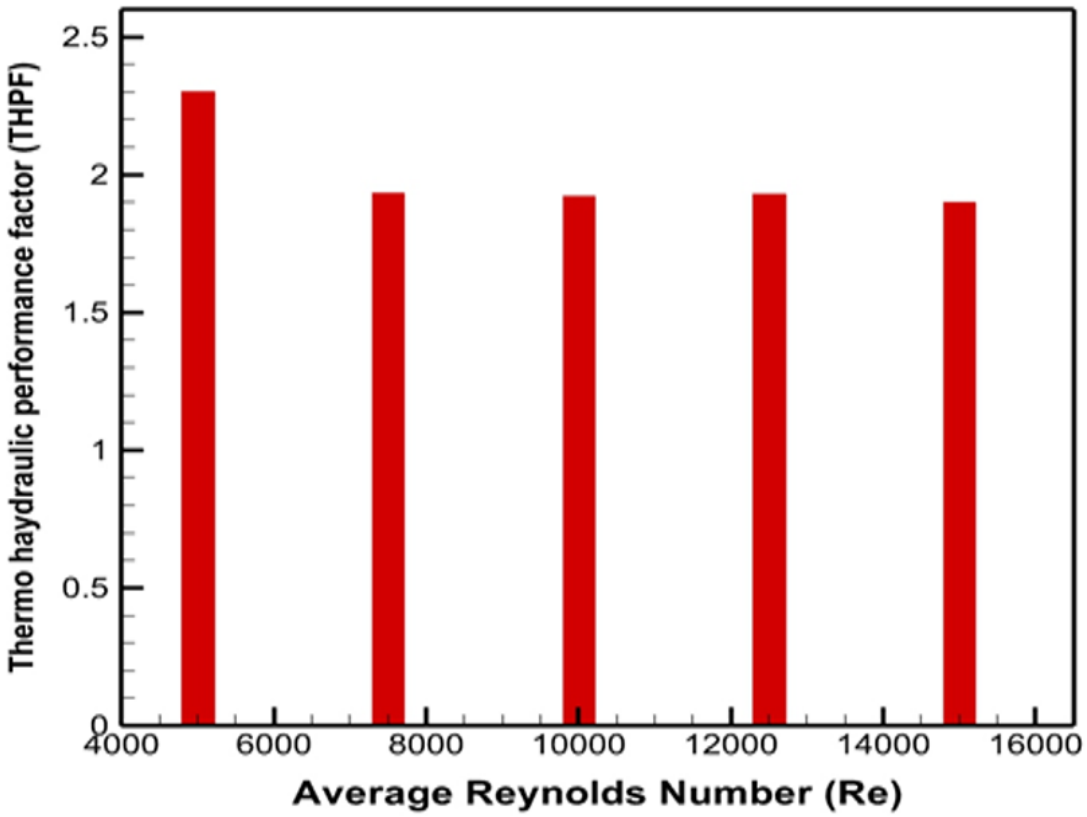

Figure 12.
Variation of the Thermohaydraulic performance factor THPF with an average Reynolds number.

5. Conclusions

Understanding and fully visualizing the flow patterns and thermal properties is important before applying a solar air heater (SAH) design. Therefore, the numerical investigation of the thermal-hydraulic performance of SAH by the presence of a spherical rib is undertaken. Several factors are studied, such as the change in the existence of spherical rib influences the Reynolds number, which is compared to a smooth surface. Each aspect is explained in detail, and the outcomes are underlined. The increase in the Reynold number (5000-15000) provides high values for the Nusselt for the smooth and spherical surface of the solar air heater. The presence of spherical ribs makes disturbances between different air layers that affect velocity vector and temperature distribution in different ranges of Reynolds numbers. The maximum enhancement of Thermohydraulic factor performance THPF is 2.3 for the Reynolds number range (5000-15000).

Maximum augmentation of the THPF factor is found at a low Reynolds number is 5000; hence, the suggested artificial roughened surface is beneficial for a low Reynolds number flow.

Edelweiss Applied Science and Technology
ISSN: 2576-8484
Vol. 9, No. 5: 2656-2669, 2025
DOI: 10.55214/25768484.v9i5.7581

Nomenclature

E is the total energy
k_{eff} is the effective thermal conductivity
S_m is a mass
$\rho\vec{g}$ The gravitational body force
k Turbulence kinetic energy.
P Static Pressure.
SΦ General source term.
$\vec{F}$ External body force.
x_i, x_j Coordinates.
∇ Gradient (vector operator).
$\bar{\bar{\tau}}$ the stress tensor.
ρ Thermal diffusivity.
$(\tau_{ij})_{eff}$ Deviatoric stress tensor.
μ Dynamic viscosity.

Transparency:

The author confirms that the manuscript is an honest, accurate, and transparent account of the study; that no vital features of the study have been omitted; and that any discrepancies from the study as planned have been explained. This study followed all ethical practices during writing.

Acknowledgments:

The writers are thankful to Electromechanical engineering Department, University of Technology, Iraq.

References

[1] M. Manjunath, K. V. Karanth, and N. Y. Sharma, "Numerical analysis of the influence of spherical turbulence generators on heat transfer enhancement of flat plate solar air heater," *Energy*, vol. 121, pp. 616-630, 2017. https://doi.org/10.1016/j.energy.2017.01.032

[2] N. Arya, V. Goel, and B. Sunden, "Solar air heater performance enhancement with differently shaped miniature combined with dimple shaped roughness: CFD and experimental analysis," *Solar Energy*, vol. 250, pp. 33-50, 2023. https://doi.org/10.1016/j.solener.2022.12.024

[3] F. O. Al Ghuol, K. Sopian, and S. Abdullah, "Enhancement of integrated solar collector with spherical capsules PCM affected by additive aluminum powder," *Journal of Thermodynamics*, vol. 2016, no. 1, p. 1604782, 2016. https://doi.org/10.1155/2016/1604782

[4] C. Prakash and R. Saini, "Heat transfer and friction in rectangular solar air heater duct having spherical and inclined rib protrusions as roughness on absorber plate," *Experimental Heat Transfer*, vol. 32, no. 5, pp. 469-487, 2019. https://doi.org/10.1080/08916152.2018.1543367

[5] A. Perwez and R. Kumar, "Thermal performance investigation of the flat and spherical dimple absorber plate solar air heaters," *Solar Energy*, vol. 193, pp. 309-323, 2019. https://doi.org/10.1016/j.solener.2019.01.014

[6] M. Sethi and N. Thakur, "Correlations for solar air heater duct with dimpled shape roughness elements on absorber plate," *Solar Energy*, vol. 86, no. 9, pp. 2852-2861, 2012. https://doi.org/10.1016/j.solener.2012.06.024

[7] R. Murmu, P. Kumar, and H. N. Singh, "Heat transfer and friction factor correlation for inclined spherical ball roughened solar air heater," *Archives of Thermodynamics*, pp. 3-34, 2020. https://doi.org/10.24425/ather.2020.132958

[8] A. K. Bhardwaj, A. Kumar, R. Maithani, R. Kumar, S. Kumar, and R. Chauhan, "Experimental study on heat transfer and fluid-flow enhancement of a spherical shape obstacle solar air passage," *Thermal Science*, vol. 23, no. 2 Part A, pp. 751-761, 2019. https://doi.org/10.2298/tsci170623220s

[9] R. Karwa, B. Maheshwari, and N. Karwa, "Experimental study of heat transfer enhancement in an asymmetrically heated rectangular duct with perforated baffles," *International Communications in Heat and Mass Transfer*, vol. 32, no. 1-2, pp. 275-284, 2005. https://doi.org/10.1016/j.icheatmasstransfer.2004.10.002

[10] A. S. Yadav, V. Shrivastava, A. Sharma, and M. K. Dwivedi, "Numerical simulation and CFD-based correlations for artificially roughened solar air heater," *Materials Today: Proceedings*, vol. 47, pp. 2685-2693, 2021. https://doi.org/10.1016/j.matpr.2021.02.759

[11] A. Ahmed, M. Ahmad, and A. Rahim, "Numerical prediction of effect on air flow rate in the presence of heated obstruction within a room," *International Review of Mechanical Engineering*, vol. 4, no. 6, pp. 702-710, 2010.

[12] S. Singh, S. Suman, S. Mitra, and M. Kumar, "Thermo-hydraulic performance enhancement of a solar air heater using rotating cylindrical turbulators," *Applied Thermal Engineering*, vol. 236, p. 121748, 2024. https://doi.org/10.1016/j.applthermaleng.2023.121748

Edelweiss Applied Science and Technology
ISSN: 2576-8484
Vol. 9, No. 5: 2656-2669, 2025
DOI: 10.55214/25768484.v9i5.7581